Van der Drift, A. C. M., Beck, H. C., Dekker, W. H., Hulst, A. G., & Wils, E. R. J. (1985) *Biochemistry 24*, 6894–6903.
Vyas, N. K., Vyas, M. N., & Quiocho, F. A. (1987) *Nature 327*, 635–638.
Walsh, K. A., & Wilcox, P. E. (1970) *Methods Enzymol. 19*, 31–41.
Yim, M. B., & Makinen, M. (1986) *J. Magn. Reson. 70*, 89–105.

Differences in the Binding of Aromatic Substrates to Horseradish Peroxidase Revealed by Fluorescence Line Narrowing†

Judit Fidy,*,‡ K.-G. Paul, and Jane M. Vanderkooi

Department of Biochemistry and Biophysics, University of Pennsylvania, Philadelphia, Pennsylvania 19104-6059, and Department of Physiological Chemistry, University of Umea, Umea, Sweden

Received February 3, 1989; Revised Manuscript Received June 2, 1989

ABSTRACT: The heme in horseradish peroxidase (HRP) isoenzyme C was replaced by mesoporphyrin (MP), and the binding effect of the aromatic substrates benzo- and naphthohydroxamic acid (BHA, NHA), resorcinol (RE), isomeric resorcylic acids (α-, β-, γ-RE), and hydroquinone (HQ) was studied at pH 5 by conventional and laser-excited fluorescence spectroscopy on the basis of the signal of the porphyrin. Under laser excitation at cryogenic temperatures site selection was demonstrated, and the fluorescence line narrowing data were used to characterize the HRP/substrate complexes by the inhomogeneous distribution function for the $S_0 \leftarrow S_1$ ($0 \leftarrow 0$) transition energy and the vibrational energies in the S_1 electronic state. A comparison with ground-state vibrational energies for MP in chloroform/ether showed a downward shift in vibrational energies for S_1 by $\approx$20 cm^{-1}. The association characteristics of the substrates were in accordance with previous literature data indicating NHA to be of the strongest binding affinity. For BHA, spectral evidence was obtained for a second type of binding site where hydrophobic interactions with the porphyrin ring may be possible. The effect of the RE's was similar to each other, but only β-RE showed saturation. Complexation in every case caused the strong reduction of the splitting in the $0 \leftarrow 0$ transition energy for the tautomeric forms of MP and an increase in the $0 \leftarrow 0$ energy by 100–200 cm^{-1} depending on the substrate. The substrate binding also affected the phonon coupling of vibronic transitions exciting into the $\Delta\nu$ = 927- and 976-cm^{-1} modes; in the latter case, the vibrational energy was also increased to 983 cm^{-1} for β-RE. In the same energy range, however, the transition into the $\Delta\nu$ = 958–960-cm^{-1} mode was not affected by binding. Both the magnitude of the energy shifting and the change in the strength of phonon coupling gave the same relation, BHA < NHA < HQ < RE's, indicating a common conformational origin. A reduction of the fluctuational freedom of the protein chain at room temperature within the heme pocket was suggested on the basis of the reduction of the width of the inhomogeneous distribution of $0 \leftarrow 0$ energies (from 60–70 to $\approx$30 cm^{-1} in case of HRP/HQ) upon substrate binding. Ways to relate the transition energy splitting and shifting effects to conformational changes are discussed by invoking the Jahn–Teller effect.

Horseradish peroxidase C2 is a heme glycoprotein, one of at least seven isoenzymes catalyzing the oxidation of indoleacetic acid and other aromatic compounds in plant roots by hydrogen peroxide. The reaction proceeds in several steps involving interactions with different hydrogen donors in the intermediate states of the enzyme. Experimental results indicate that the native enzyme forms a 1:1 complex with aromatic donor molecules and that different substrates bind at the same site within the heme crevice (Schoenbaum, 1973; Leigh et al., 1975; Schejter et al., 1976; Paul & Ohlsson, 1978; Morishima & Ogawa, 1979). In these works it was also suggested that the binding of the aromatic donors involves hydrophobic interaction with aromatic residues of the protein and that the donor is at a distance of 5.8–11.2 Å from the center of the heme. However, the binding site and the nature and geometry of the binding process have not yet been identified. The most recent studies, performed by NMR spectroscopic techniques and computer simulation procedures, revealed that the binding site involves a tyrosine residue in the vicinity of the porphyrin peripheral 8-methyl (Sakurada et al., 1986) and 7-propionate (Thanabal et al., 1987) groups; however, these results somewhat contradict the model based on resonance Raman data (Oertling & Babcock, 1988).

Although a series of results showed somewhat uniform behavior in the binding of a great number of ligands, difference absorption measurements indicated different types of changes in the Soret band of the heme due to binding of various substrates. To help understand the reason for this, two categories were suggested (Sakurada et al., 1986), represented by resorcinol and 2-methoxy-4-methylphenol, respectively, but not all published results seem to fit into this picture [e.g., see Schoenbaum (1973)].

In recent years, we have successfully applied the high-resolution laser spectroscopic technique, fluorescence line narrowing, for small monomeric heme proteins, and experimental evidence was presented and discussed for the fulfillment of the

† This work was supported by NIH Grant GM 34448 and by Swedish Research Council Grant B89-3X-7130.
* Address correspondence to this author.
‡ On leave from the Institute of Biophysics, Semmelweis Medical University, H-1088, Puskin utca 9, Budapest, Hungary.

0006-2960/89/0428-7531$01.50/0

site selection condition especially for cytochrome *c* and horseradish peroxidase (Angiolillo et al., 1982; Horie et al., 1985; Vanderkooi et al., 1985; Koloczek et al., 1987; Fidy et al., 1987, 1989). For our present spectroscopic studies, we have replaced the prosthetic group (ferric protoporphyrin IX) of horseradish peroxidase (HRP)[1] by mesoporphyrin IX (MP). In the earlier studies (Horie et al., 1985) it was shown that the substituted enzyme maintains its substrate binding ability. We have found the free base MP substitution especially useful for characterizing the heme crevice, as the two pyrrole hydrogen tautomers of MP were found to be distinguished spectroscopically and their spectroscopic properties were very sensitive to conformational changes within the pocket (Fidy et al., 1987, 1989). Moreover, the inhomogeneous distribution of the $0 \leftarrow 0$ transition energy for the chromophores was found to be rather narrow, 60–70 cm^{-1}, which not only demonstrated the proper reconstitution of the protein but also made it possible to resolve fine details such as splittings in electronic energy or the presence of different species in the system.

In this work, we study the binding of benzo- and naphthohydroxamic acids (BHA, NHA), resorcinol (RE), isomeric resorcylic acids (α-, β-, γ-RE), and hydroquinone (HQ), making use of our previous findings on the spectroscopic properties of MP-HRP. The results gained by laser spectroscopy at cryogenic temperatures in comparison with conventional room temperature and low-temperature (77 K) spectroscopic measurements clearly demonstrate the advantages of the high-resolution technique that made it possible to distinguish different types of conformational effects for the resorcinol-type molecules, the hydroxamic acids, and hydroquinone.

Materials and Methods

Mesoporphyrin horseradish peroxidase isoenzyme C was synthesized as described (Vanderkooi et al., 1985). Benzohydroxamic acid was from Aldrich Chemical Co. (Milwaukee, WI). Naphthohydroxamic acid was synthesized in Dr. G. R. Schoenbaum's laboratory (St. Jude Children's Research Hospital, Memphis, TN) and kindly donated for our purposes. Resorcinol, the resorcylic acids, and hydroquinone were from Sigma Chemical Co. (St. Louis, MO). The structures of the substrates are shown in Figure 1A and that of mesoporphyrin IX in Figure 1B. The samples were prepared in 50 mM ammonium acetate, pH 5, in micromolar concentrations, and 50% of glycerol was added when low-temperature measurements were performed. Ligand solutions of great reactivity with oxygen were prepared under argon protection.

Conventional fluorescence measurements were performed by a Perkin-Elmer LS5 spectrofluorometer. For the site selection measurements a continuous wave argon ion–Rhodamine dye laser system (Coherent, Palo Alto, CA) was used as the tunable laser source for excitation, and the emission spectra were registered through a JY Ramanor HG2 double holographic monochromator (Koloczek et al., 1987). The resolution of the laser spectrophotometer was 1 cm^{-1}. Low temperature was achieved by using an EPR liquid helium Dewar (Air Products, Allentown, PA) or a Dewar filled with liquid nitrogen.

In interpreting the spectral results, we strongly relied on the definition and determination of site distribution functions for the different substrate-bound cases. Site distribution was understood as the inhomogeneous distribution of the chromophores caused by the fluctuations (conformational flexibility) of the protein at room temperature. The samples during cooling to cryogenic temperatures undergo structural relaxations, but still maintain a distribution of conformational substrates at low temperature [e.g., Frauenfelder and Young (1986) and references cited therein]. The population of chromopohores surrounded by slightly different conformations is represented spectrally in a distribution of transition energies ("spectral" distribution). The fluorescence site selection technique has that unique characteristic that it allows for the direct determination of this distribution, proving thus the existence of substates. The method for the determination of site distribution functions was first proposed by Fuenfschilling et al. (1981, 1982), and we used it as it follows.

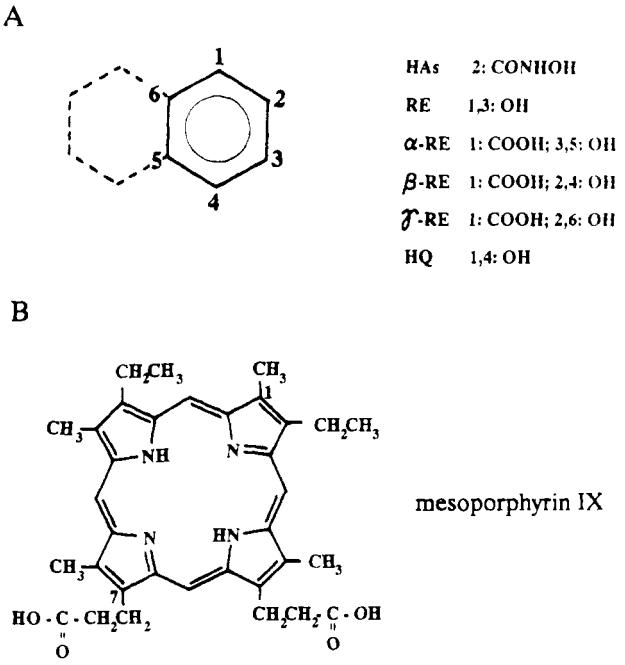

FIGURE 1: Schematic representation of (A) substrate structures (from the HA's, full lines apply to BHA, while for NHA, the figure is completed by the dashed part) and (B) mesoporphyrin. Ring C atoms and joined H atoms are not indicated.

The measured emission spectrum, $I(E_{ex},E_{em})$ excited at a laser energy of E_{ex}, in general, originates from all kinds of conformational situations (sites) in the sample, where excitation could be achieved by the chosen energy; i.e.

$$I(E_{ex},E_{em}) = \int \epsilon(E_{ex} - E_i)n(E_i)f(E_i - E_{em})\,dE_i \quad (1)$$

where ϵ and f are the absorption and emission spectra for the excitation and emission processes, respectively, E_i is the characteristic $0 \rightarrow 0$ transition energy for the ith site, and $n(E_i)$ is its site distribution function. This formula involves the approximation that the chromophores among the slightly different conformational conditions still maintain the same Franck–Condon factors, vibrational energies, and phonon wing contributions (Fuenfschilling et al., 1981, 1982). If now we only consider the sharp zero phonon emission lines in the spectrum, it follows from formula 1 that sharp emissions will occur only when both ϵ and f are represented by sharp zero phonon lines. This happens when $E_{ex} - E_i$ equals a vibrational energy (E') in the excited state and $E_i - E_{em}$ equals a vibrational energy (E) in the ground state. In this case the convolute in formula 1 will be replaced by a much simpler expression:

$$I = K\epsilon(E')n(E_{ex} - E')f(E) \quad (2)$$

where K is a constant. Our measurements and calculations

[1] Abbreviations: HRP, horseradish peroxidase; BHA, benzohydroxamic acid; NHA, naphthohydroxamic acid; HQ, hydroquinone; RE, resorcinol.

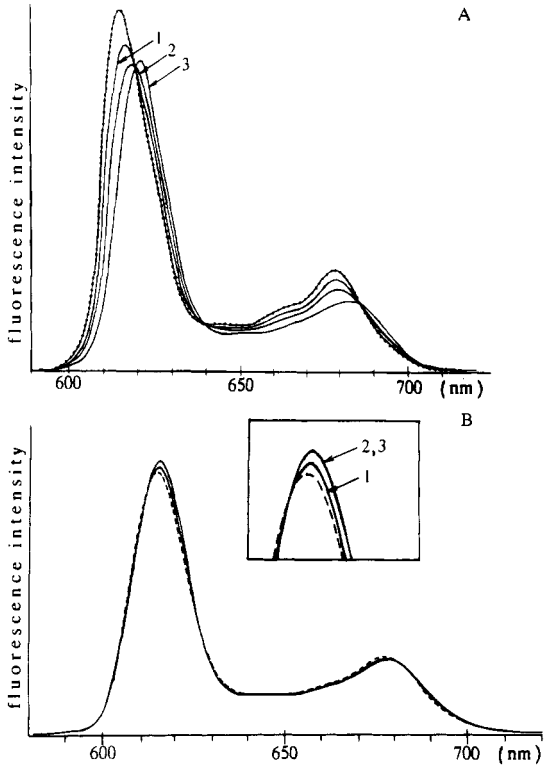

FIGURE 2: Room temperature fluorescence spectra of (A) 4.7 μM MP-HRP excited at 400 nm (dotted line) and the same sample when 2.4 μM NHA (curve 1), 9.9 μM NHA (curve 2), and 25.4 μM NHA are added (curve 3) and (B) 0.46 μM MP-HRP excited at 400 nm (dashed line) and the same sample when 3.6 mM β-RE (curve 1), 7 mM β-RE (curve 2), and 12 mM β-RE are added (curve 3). The region of band maxima is also shown magnified in the inset.

concerning $n(E_i)$ were based on formula 2. We varied E_{ex}, and from each measured spectra we picked up that sharp $0 \leftarrow 0$ emission line ($E = 0$) that originated from the same vibronic excitation ($E' =$ constant). Fixing thus both E and E' in the formula, the measured line intensities in function of the excitation energy follow the functional form of the distribution function:

$$I = K'n(E_{ex} - E') = K'n(E_i) \quad (3)$$

where K' is a constant. The measured $n(E_i)$ values were then fitted with Gauss distribution function $n(E_i) \approx \exp\{-(E_i - \mu)^2/2\sigma^2\}$, and the mean value of $0 \leftarrow 0$ transition energy (μ) and the width (2σ) of the distribution were used as characteristic values. One evidence for the site selection condition is the experimental determination of the site distribution function, which should be independent of the vibronic mode chosen for the measurement. The fulfillment of this requirement for MP-HRP was presented and discussed earlier (Fidy et al., 1987, 1989).

RESULTS

Broad-Band Excitation Methods

Room Temperature Measurements. In Figure 2 the room temperature fluorescence spectrum of MP-HRP excited at 400 nm is shown by a dashed line, and its change when an increasing amount of NHA (Figure 2A) or β-RE (Figure 2B) are added is shown by solid line. The spectral change for NHA binding is in accordance with our previous results on the same system (Vanderkooi et al., 1985). Because of the high activity of HQ toward oxidation, room temperature measurements for that case were not performed. Binding of the substrate causes a red shift in the emission spectrum in both cases; the emission intensity decreases in the case of NHA and slightly increases

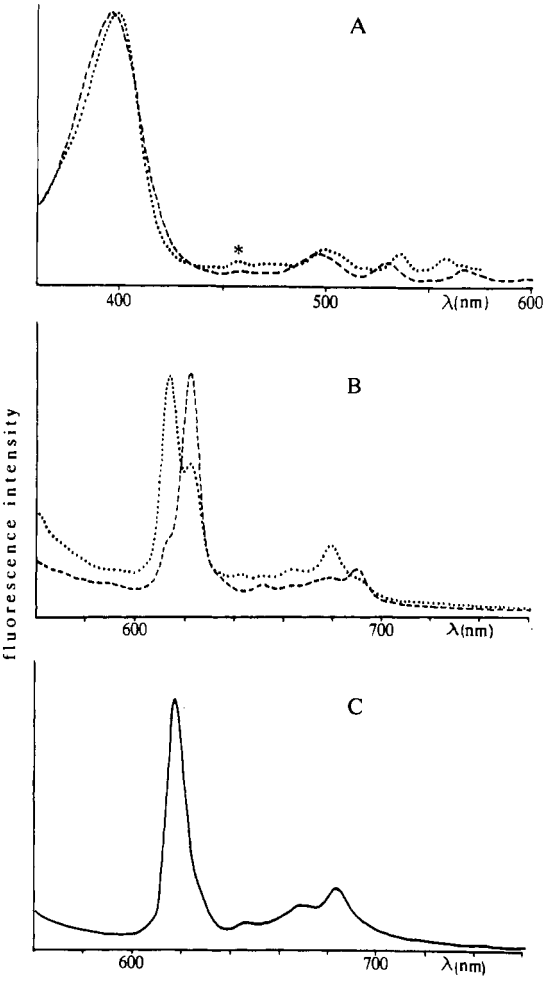

FIGURE 3: Fluorescence spectra of 4.2 μM MP-HRP at 77 K with a slit width of 3 nm. (A) Fluorescence excitation spectra for the two tautomeric forms of MP-HRP; emission measured at 610 nm (dotted line) and 625 nm (dashed line), respectively. (The peak designated by an asterisk is an experimental artifact.) (B) Fluorescence emission spectra for the two tautomeric forms of MP-HRP; fluorescence is excited at 538 nm (dotted line) and 528 nm (dashed line), respectively. (C) Fluorescence emission spectrum after addition of 100 μM NHA. The curve represents two identical emission spectra when excited at 538 and 528 nm.

for β-RE, leading to saturation as curves 3. The spectral changes are very similar to the NHA case when BHA is added; however, the concentration relations are different, indicating a significant difference in the dissociation constants as $k_d^{BHA}/k_d^{NHA} \approx 10$ in accordance with literature data (Schoenbaum, 1973). There is also a small difference in the final spectrum of the complexed form; in the case of BHA, the spectrum resembles curve 2 more than curve 3. RE and α- and γ-RE were similar to β-RE in terms of spectral shifts (data not presented), but their estimated k_d values were higher possibly due to their low pK values. RE and α-RE lead to 5% and 10% of the intensity decrease, respectively, until saturation (for spectral changes); however, γ-RE effectively quenches, and it does not reach saturation up to a concentration of 7 mM (added to 0.2 μM HRP). In accordance with previous data for native HRP (Ohlsson et al., 1986), we found k_d significantly bigger in the case of resorcinols than for the hydroxamic acids. The relation in binding ability is then NHA > BHA $\gg$ RE's.

Measurements at 77 K. Low temperature produces higher resolution in the spectra. In Figure 3 the effect of binding is demonstrated in the case of NHA at 77 K. Parts A and B refer to the excitation and emission spectra of the free protein,

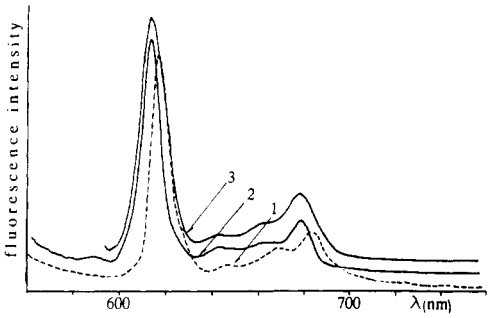

FIGURE 4: Fluorescence spectra of MP-HRP excited at 400 nm at 77 K: 4.7 μM protein + 25 μM NHA (curve 1), 2.4 μM protein + 22 mM β-RE (curve 2), and 4.3 μM protein + 25 mM HQ (curve 3).

respectively, and part C corresponds to a sample saturated with NHA. The spectra shown in parts A and B of Figure 3 by dotted and dashed lines were proven to originate from the two inner-ring tautomeric forms of MP in HRP (Fidy et al., 1987), respectively, and thus allow for the comparison of the tautomers. The two tautomeric spectra are normalized for the same maxima on each figure; however, at room temperature the form represented by the dashed line is only present in the samples by less than 5% at pH 5 (Fidy et al., 1987), leading to a fluorescence emission dominated by the majority tautomer as seen in Figure 2. In Figure 3A we can see that in the Soret band there is only a small spectral difference between the tautomers, but the difference becomes more significant within the Q bands. This spectral difference allows for selective excitation and leads to the emission spectra shown in Figure 3B. The main emission peaks at 613 and 622 nm thus characterize respectively tautomer 1 and tautomer 2 [nomenclature is after Gurinovich et al. (1986), where 1 refers to the majority tautomer form]. Due to the binding of NHA the duality of the emission spectra disappears; by use of the specific excitation frequencies where the tautomeric forms can be distingiushed for the free protein, they lead to identical emission spectra for the complexed form (Figure 3C). This new single emission spectrum is shifted to the red from that of the original form 1 tautomer (dotted line on Figure 3B), and it is blue shifted from that of the other form. These measurements at 77 K elucidate the room temperature spectral changes shown in Figure 2: the spectrum, dominated by the majority tautomer component for free protein is changing into a spectrum characterized by only one peak, red shifted from that of the majority tautomer, when substrates are added.

In Figure 4 the emission spectra excited at 400 nm for MP-HRP/β-RE (curve 2) and MP-HRP/HQ (curve 3) complexes are compared to the MP-HRP/NHA case (curve 1, shown also in Figure 3). The difference is striking between the NHA case and the other two; the main maximum is at 618 nm, while that for the others is at 614 nm, almost identical with that (613 nm) of the majority tautomer form in the free protein. The effect is similar in that substrate binding diminishes the spectral separation of the tautomeric MP forms. The main emission band in the HQ case is much broader than with β-RE, but this sample was shown to still contain a large amount of the substrate-free protein, which also significantly contributes to the spectrum by both tautomeric emissions when excited at 400 nm.

Laser Excitation Technique

Fluorescence Line Narrowing Spectra. The fluorescence site selection spectrum of the free protein at 22 K is presented in Figure 5A. The sharp emission lines at higher energies than 15900 cm^{-1} originate from 0 ← 0 emissions of those MP

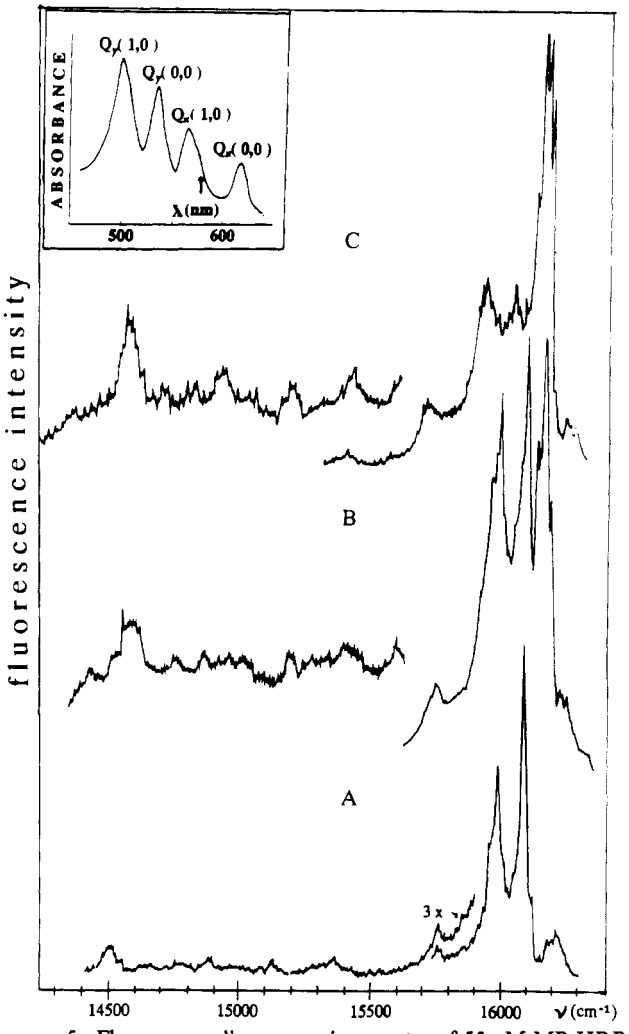

FIGURE 5: Fluorescence line narrowing spectra of 55 μM MP-HRP after equilibrium was reached under excitation by 17310 cm^{-1} (577.7 nm) at 22 K. The region for emissions to higher ground-state vibrational levels is 3× magnified. (A) Free protein, (B) free protein with 120 μM NHA added, and (C) free protein with 300 μM NHA added. Inset: Room temperature absorption spectrum of MP-HRP in the region of the O_x and O_y bands. An arrow indicates the excitation energy used in the line narrowing experiments.

molecules that can be excited by 17310 cm^{-1} (through any kind of vibronic excitation within S_1). The emission lines found toward lower energies originate from transitions between the lowest vibronic level in S_1 to the higher vibrational levels in S_0 ($\nu \leftarrow 0$), as discussed elsewhere (Koloczek et al., 1987). It was also shown that, at this temperature, both MP tautomeric forms are populated, and among the 0 ← 0 emissions, the one seen in the figure at 16100 cm^{-1} corresponds to tautomer 1 while that at 16000 cm^{-1} represents tautomer 2. It is interesting to note that this spectral separation of 100 cm^{-1} is significantly smaller than was observed by the conventional peak separation in Figure 3 and 77 K: 9 nm $\approx$ 236 cm^{-1}.

The addition of NHA leads to the appearance of new emission lines within a narrow energy range between 16100 and 16200 cm^{-1} (Figure 5B); their relative intensity increases upon addition of more substrate (compare parts B and C of Figure 5). In the saturated case, shown in Figure 5C, the sharp 0 ← 0 emission lines for the tautomers of the free protein completely disappear and only the new, complexed form is represented by definitely higher energy emissions. Upon binding, an increase in emission intensity in the range of $\nu \leftarrow 0$ emissions can also be observed. The energy of these lines related to the position of the intense 0 ← 0 lines does not

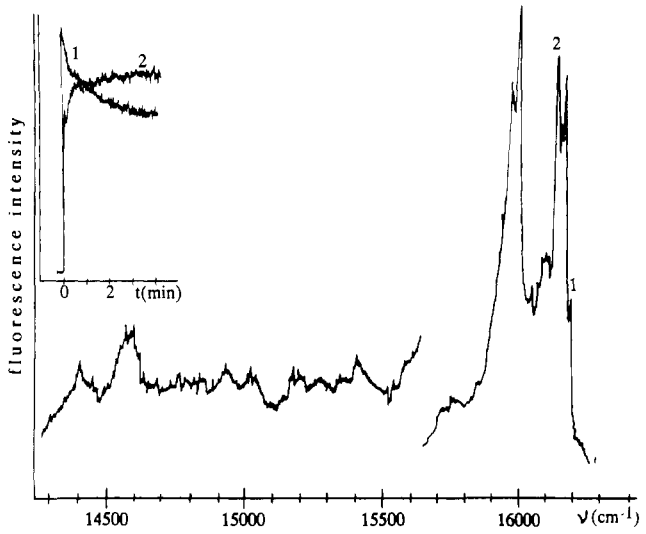

FIGURE 6: Fluorescence line narrowing spectrum of the sample described in Figure 5B with an excitation of 17 310 cm^{-1} at 4.8 K. Inset: Emission intensity change during irradiation at 17 310 cm^{-1} in a sample heat-treated at 70 K for 5 min and then cooled to 4.8 K, where irradiation was started. The intensities were corrected for background. Curve 1 represents the intensity of peak 1 at 16 200 cm^{-1}; curve 2 is that of peak 2 at 16 145 cm^{-1} in a function of irradiation time.

change; they are only shifted together with the new position for the bound case. In figure 5B we can see that this part of the spectrum is the sum of the two corresponding parts in A and C of Figure 5 due to the mixed nature of this system.

To demonstrate the relation between tautomeric forms and emission lines, we performed a photoreaction experiment at 4.8 K on the same sample, which was characterized by the spectrum in Figure 5B at 22 K. Before irradiation, the sample was heated to 70 K where, in the free protein, only tautomer 1 was shown to be populated (Fidy et al., 1989). The sample was then adjusted to 4.8 K, and phototautomerization was started under the influence of the exciting light (Fidy et al., 1987, 1989) in which form 1 (emission at 16 100 cm^{-1}) is transformed into form 2 (emission at 16 000 cm^{-1}) within the site excited. In Figure 6 we show the equilibrium spectrum of the sample at 4.8 K. It is seen that, after irradiation, only tautomer 2 is represented by its emission in the region of the free protein emission lines. In the range of the 0 ← 0 emissions for the complexed form, some phototransformation can also be seen at lines 1 and 2. In the inset, the time course of these line intensities shows a conversion from one type to another. Similar conversion types of changes were also detected in cases when β-RE and HQ were added.

In Figure 7 the effect of the different substrates on the line narrowing spectra in the range of the 0 ← 0 emissions is compared, with excitation at 17310 cm^{-1}. In some of the spectra, some amount of free protein is represented by the tautomer emissions at 16 100 cm^{-1} (marked by 1) and 16 000 cm^{-1} (marked by 2). Binding can be saturated in the case of NHA (Figure 7B) and β-RE (Figure 7D). The spectrum for added BHA is almost identical with the NHA case in the position of the new 0 ← 0 lines above 16 100 cm^{-1}, but with BHA, full complexation cannot be achieved. HQ seems to be the least effective in binding (Figure 7C); the intensity mainly comes from the free protein emissions, though the appearance of new emission bands is evident (compare with the spectrum in Figure 5A). RE and α- and γ-RE also did not lead to the saturation of the binding sites; the position of the new lines for complexed molecules was identical with that of the shown β-RE case. The new 0 ← 0 energies corresponding to the complexed molecules seem to appear in different ranges for the HA's, HQ, and RE's, having higher and higher energies related to the free case. This tendency in the binding effect of different substrates was indicated also by the conventional spectroscopic measurements (Figure 4) in the cases of NHA and β-RE, where the emission spectra could be attributed solely to complexed molecules. In the other cases, complexed and free proteins could not be spectrally separated, and thus the information remained hidden.

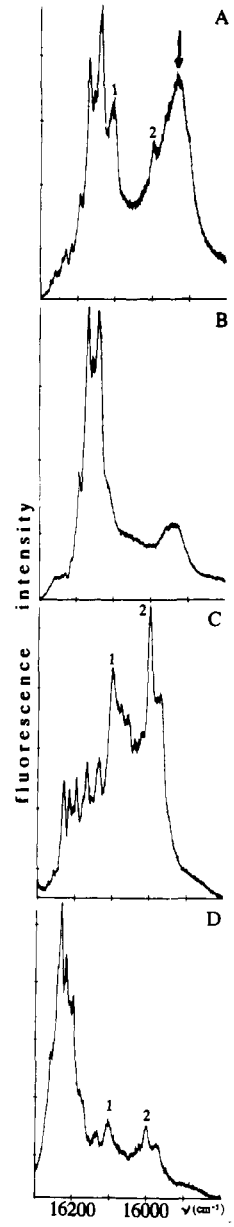

FIGURE 7: Fluorescence line narrowing spectra of MP-HRP/substrate complexes when excited at 17 310 cm^{-1} at 20 K: (A) sample complexed with BHA; (B) sample saturated with NHA; (C) sample complexed with HQ; (D) sample saturated with β-RE. The emission lines designated by 1 and 2 are those of free MP-HRP tautomeric forms 1 and 2, respectively.

The effect of NHA and BHA on the spectrum of MP-HRP can be compared in parts B and A of Figure 7, respectively. A new unresolved strong band can be seen for BHA around 15 920–15 930 cm^{-1} (indicated by an arrow in Figure 7A), which is also present for NHA but represented by much less emission intensity. The appearance of this structureless emission for BHA is readily detectable even at low concentrations.

Site Distribution Functions. The spectra, measured at a series of excitation energies, can be used to determine the site

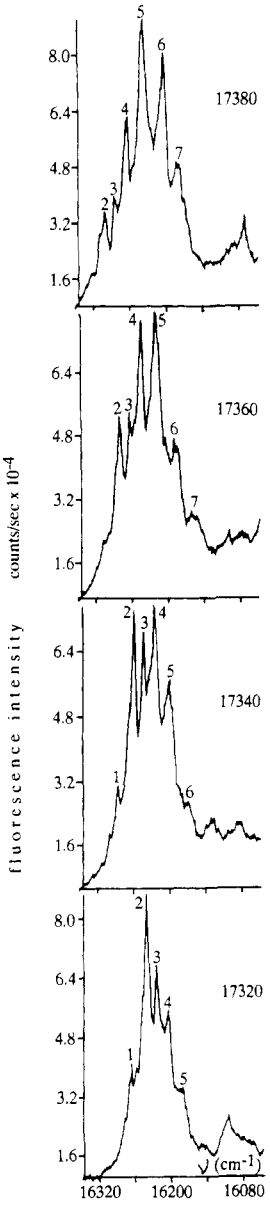

FIGURE 8: Evidence for site selection in the fluorescence line narrowing measurement for β-RE-bound HRP complexes at 25 K: 0 ← 0 emission line intensities and energies changing due to varying excitation energy as indicated in cm^{-1} on the spectra. The 0 ← 0 emission lines marked by numbers from 1 to 7 originate from those protein molecules that are excited through their $\Delta\nu$ = 1051-, 1080-, 1095-, 1114-, 1139-, 1175-, and 1195-cm^{-1} vibronic levels in their S_1 states, respectively.

distribution functions of systems (described under Materials and Methods). The change in the range of 0 ← 0 emissions is shown for MP-HRP complexed with β-RE in Figure 8 for a series of excitation energies as indicated. (For the actual determination of site distribution functions, the excitation energy was changed in steps of 10 cm^{-1}.) In the evaluation process, the intensity of the emission line appearing by a given (vibrational) energy below the excitation energy (marked by a given number in Figure 8) was determined for each excitation energy. The data corrected for the excitation intensity were plotted against the emission energy and averaged for measurements performed by excitations through different vibronic levels (see Materials and Methods). The data points are shown in Figure 9, together with fitted Gauss distribution functions represented by full lines. The functions finally correspond to the probability of finding chromophores in the system characterized by a given 0 ← 0 energy. The parameters of the fitted functions are shown in Table I.

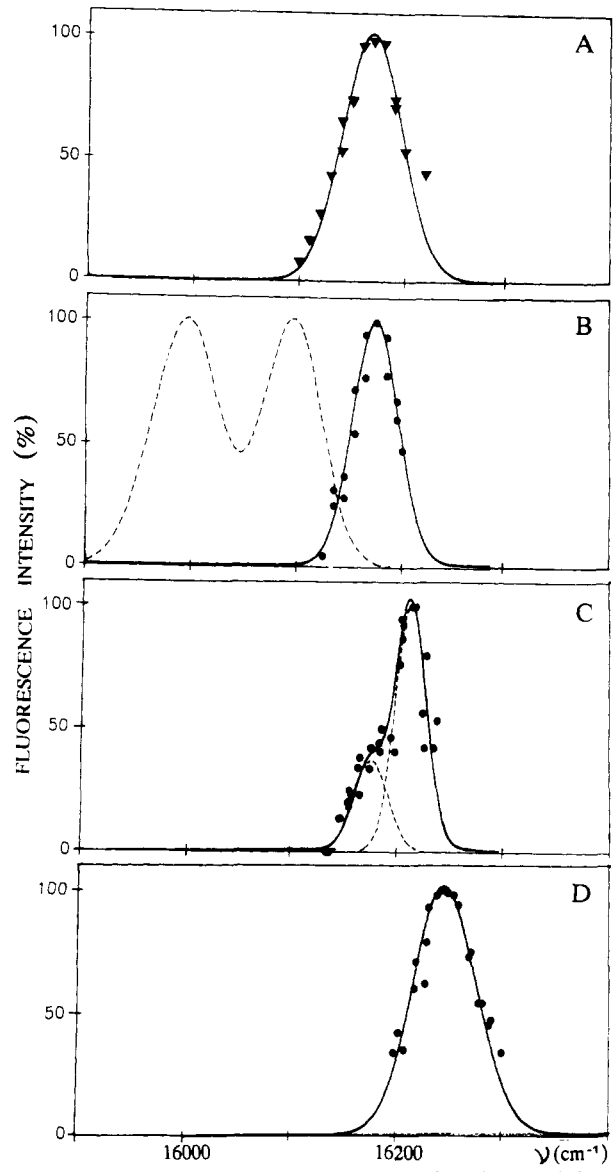

FIGURE 9: Data points for site distribution functions and fitted Gaussian distribution functions for MP-HRP/substrate complexes at 20 K. On the abscissa, 0 ← 0 emission energies are indicated; the normalized intensity values shown on the ordinate correspond to the probability of finding complexed proteins with a given 0 ← 0 energy in the sample. For the measurements, the excitation energy was varied between 17 200 and 17 400 cm^{-1}, and the plotted data are mean values of data for three to five vibrational modes between $\Delta\nu$ = 1050 cm^{-1} and $\Delta\nu$ = 1150 cm^{-1}. The parameters of the fitted functions are given in Table I. (A) MP-HRP/BHA; (B) MP-HRP/NHA [the double maximum curve shown by the dashed line is the distribution function for free MP-HRP (Fidy et al., 1987)]; (C) MP-HRP/HQ; (D) MP-HRP/β-RE.

Table I: Parameters of Gauss Fitting to Site Distribution Functions, Mean 0 ← 0 Energy (μ) and Width of Distribution (2σ), and Conventionally Measured Band Maximum Positions for 77 K (E^{77K}) with Corresponding μ Values Shown in Parentheses

	μ (cm^{-1})		2σ (cm^{-1})		E^{77K} (nm)	
system	taut 1	taut 2	taut 1	taut 2	taut 1	taut 2
free MP-HRP	16100	16000	60	70	613 (621)	622 (625)
+BHA	16168		56			
+NHA	16175		43		618 (618.2)	
+HQ	16215	16175	28	32		
+β-RE	16245		60		614 (615.6)	

In Figure 9B, the site distribution function for free MP-HRP can also be seen represented by a dashed line. The two

Table II: Vibrational Energies (in cm^{-1})[a] for the S_1 State of MP in Different HRP Systems[b] and Vibrational Energies, Assigned Modes, and Symmetries for $(Imidazole)_2Fe^{III}$–MP Complexes in the Corresponding Region by Choi and Spiro (1983)

free MP-HRP					
taut 1	taut 2	NHA bound	HQ bound	β-RE bound	$(ImH)_2Fe^{III}$–MP
724					
760					
810		815		810	
883 (PW)		889 (PW)		886 (PW)	846, C_mH
910 (sPW)		912 (sPW)	912 (sPW)	911 (sPW)	951 (939)*, C_bS, E_u
926 (sPW)		927 (sPW)	927 (sPW)	927 (PW)	
960		958	958	959	981 (973)*, A_{1g}
968		968 (sPW)	968 (sPW)	969 (sPW)	1001, C_aN, E_u
976		976 (sPW)	976 (sPW)	983 (sPW)	
1038		1040	1040	1039	
1051	1051	1052	1051	1052	
1060 (w)	1060 (w)	1062 (w)	1062 (w)	1061 (w)	
		1072 (w)	1070 (w)	1072 (w)	
1080	1080	1081	1081	1081	
1095	1093		1093	1094	
1115	1112		1114	1112	
1145	1145		1142	1139	
			1169 d		
1178	1176		1176 d	1176	
1210	1207		1207 d		
1236	vw				
1258	1258				
1271	1271				
1290	1290				
1312	1311				
1324	vw				
1348	1346				
1367	1366				
	1378				
	1387				
	1410				
	1450				

[a] The standard error is 1 cm^{-1} and for weak (w) or phonon wing (PW) bonds is 1.5 cm^{-1}. [b] Abbreviations: vw, very weak; sPW, significant phonon wing contribution; d, doublet; *, data for Fe^{II} complexes.

maxima seen correspond to the two tautomeric forms, which in this system have very different characteristic (mean) $0 \leftarrow 0$ energies (Fidy et al., 1987, 1989). Looking at the functions representing the protein complexed with different substrates, we can see that all binding types cause higher emission energies than that of the free molecule and that the energies are significantly different for each case. The relation concerning the magnitude of mean $0 \leftarrow 0$ energies is RE's > HQ > HA's > free MP-HRP. The effect of NHA and BHA on the mean $0 \leftarrow 0$ energy is almost the same; however, the distribution function for BHA is broader. We see also that in only the case of HQ can we resolve the function for two components, which might represent the two tautomeric forms of MP. (Because of the presence of a large amount of substrate-free protein in these samples, the distribution function for the complexed form was determined after subtracting the overlapping tail of that for the free molecules.) In the other cases, we see either only one type of tautomeric forms populated or the resolution for the tautomeric forms hindered by the width of the distributions. In fact, the HQ-bound case shows outstandingly narrow distributions (see Table I), which may contribute to the appearance of resolution. The minority component shows remarkable agreement with the position of the distribution for the NHA complexed form (Figure 7B); it is possible that between these two cases the difference originates solely from population differences for the same tautomeric forms.

Vibrational Energies for the S_1 State. It is known that the $\nu \leftarrow 0$ emission region in fluorescence site selection spectra (energies below 15900 cm^{-1} in Figure 5A) contains information on ground-state vibrational levels (appearing in resonance Raman spectroscopy), while the $0 \leftarrow 0$ part of the spectra, when measured by using a series of excitation energies, can be used to determine a wide range of vibrational energies for those electronic energy levels, where the vibronic excitation took place (Personov, 1983). Vibrational energies for the S_1 state are given in Table II as the difference between the exciting energy and the emission energies detected as $0 \leftarrow 0$ transitions (e.g., see Figure 8) and are expected to be somewhat smaller than those for the ground state. The energy range where data could be determined is limited by the energy range where excitation could be performed by our laser source and by the relation of this energy range to the absolute value of $0 \leftarrow 0$ energies. The uncertainty (standard error) of the data is ± 1 cm^{-1} in general, originating mainly from the reproducibility error of the excitation wavenumber. For lines largely affected by phonon interactions, or of low intensity, the error is higher: ± 1.5 cm^{-1}.

As seen in Table II, only a few differences in vibrational energies between the various HRP systems are observed. There is a weak line at $\Delta\nu$ = 1070–1072 cm^{-1} that appears only for the substrate-bound cases, and a new line was found at $\Delta\nu$ = 1169 cm^{-1} for the HQ bound case as a doublet component for the 1176-cm^{-1} line. In this latter case, the line for $\Delta\nu$ = 1207 cm^{-1} also shows a doublet-like character. As discussed under Materials and Methods, the emission spectrum is a convolution integral of the absorption and emission spectra and the site distribution function; thus in this technique, it is hard to determine the intensity relations precisely (except evidently large intensity differences) among the true emission lines. There are differences in the shape of the emission lines, however. This is demonstrated in Figure 10, where $0 \leftarrow 0$ emission lines are shown originating from $\Delta\nu$ = 912 cm^{-1} (line 1), $\Delta\nu$ = 927 cm^{-1} (line 2), $\Delta\nu$ = 958 cm^{-1} (line 3), and $\Delta\nu$ = 968 cm^{-1} (line 4) vibronic excitations for the systems MP-

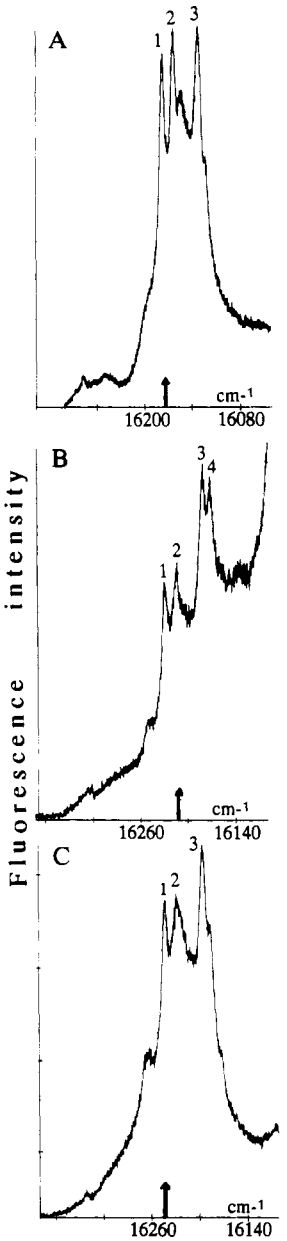

FIGURE 10: Fluorescence line narrowing spectra for $0 \leftarrow 0$ emission lines originating from $\Delta\nu$ = 914 cm^{-1} (line 1), $\Delta\nu$ = 927 cm^{-1} (line 2), $\Delta\nu$ = 958 cm^{-1} (line 3), and $\Delta\nu$ = 968 cm^{-1} (line 4) vibronic excitation for MP-HRP/substrate complexes. (A) NHA complexes excited at 17090 cm^{-1}, 10 K; (B) HQ complexes excited at 17140 cm^{-1}, 13.5 K; (C) β-RE complexes excited at 17155 cm^{-1}, 6 K. Arrows on the abscissa indicate the position of the distribution functions for $0 \leftarrow 0$ energies.

HRP/NHA (Figure 10A), MP-HRP/HQ (Figure 10B), and MP-HRP/β-RE (Figure 10C), respectively. Arrows on the energy scale show the mean $0 \leftarrow 0$ transition energy as determined from the site distribution functions. In Figure 10A, between lines 2 and 3 we see a broad, lower intensity band which can be identified as the sum of the phonon contribution (phonon wing = PW) to the zero phonon lines (ZPL) seen as 2 and 3 (Personov, 1983). If we follow the appearance of the lines in the different systems, we find that, in the HQ-bound case, line 2 has a decreased ZPL intensity relative to the PW band of the transition, and in the β-RE-bound structure, the $\Delta\nu$ = 927-cm^{-1} transition has lost almost completely its ZPL intensity and the emission intensity appears mainly within the broad PW band. In Table II we can see another difference in the PW contributions. In the substrate-bound cases, the lines for $\Delta\nu$ = 968 and 976 cm^{-1} show more significant PW contributions than those for the free protein, and for β-RE, it is also shifted to 983 cm^{-1}.

Discussion

Change in Energy Splitting for Tautomeric Forms. van der Waals and his co-workers (Voelker & van der Waals, 1976) used the Jahn–Teller theory of vibronic interactions (Jahn & Teller, 1937; Bersuker, 1984; Bersuker & Stavrov, 1988) to interpret the matrix-dependent energy separation of the tautomeric forms of a free base porphyrin. According to their model, the tautomeric forms of a symmetric free base porphyrin (e.g., porphin) are coupled through vibronic interactions, which leads to energy separation if the surrounding matrix has an electric potential of special asymmetry within the plane of the molecule. On the basis of our results for MP-HRP (Fidy et al., 1989), we suggested extending the theory for this system as well and found the tautomeric splitting and the excited-state energies of MP extremely sensitive to the electric potential in the plane of the molecule. In the present study, the phototransformation experiments (see Figure 6) indicated that, not only in the case of HQ but also for the other substrate-bound cases, both tautomeric forms are present within the distributions, but with closely lying transition energies. Thus we see that the energy separation of the tautomeric forms in the substrate-bound cases is strongly reduced (becomes hindered by the width of the site distribution) compared to the free case. The splitting value can be estimated from the HQ case (Table I) where the narrow distributions and difference in their maximum values allow for the determination of ΔE as $\approx$40 cm^{-1}. This value is not much higher than that expected only on the basis of the asymmetry of the MP molecule itself (Hoffman & Ratner, 1978).

The change in the energy separation due to substrate binding can be interpreted in two ways. (1) A conformational change took place in the heme pocket so that the planar asymmetry of the crevice potential became reduced. (2) The porphyrin molecule became distorted so that it has lost its symmetry prerequisite for energy splitting through Jahn–Teller effect. The latter conclusion is in accordance with NMR data (Morishima & Ogawa, 1979), which showed that a local conformational change involving peripheral methyl groups takes place upon substrate binding to native HRP. Other magnetic resonance data (Leigh et al., 1975) also indicated that substrate binding may strongly affect the planarity of the heme. In our measurements, the increased probability for $\nu \leftarrow 0$ transitions seen in Figure 5 for complexed molecules is a sign for distortion of the porphyrin ring upon binding. Thus we think both effects to be important.

Width of Site Distributions. Considering the fact that in all substrate-bound cases we probably see the envelope of two closely lying distributions for the tautomeric forms, we see that substrate binding leads to the narrowing of these functions (see data in Table I). In interpreting this effect, we consider that these detected distributions were formed by structural relaxations from room temperature during a cooling time of $\approx$10 s. It is reasonable to suppose that the resulting conformational distribution at low temperature is not independent from the motional freedom and flexibility of the room temperature form. Thus, when binding resulted in a narrowing for the site distribution functions, we think it meant that a reduction of protein fluctuations in the vicinity of the heme occurred at room temperature as well. This effect is the most evident for HQ, which showed the narrowest distribution ever reported for a heme protein.

Change in $S_0 \leftarrow S_1$ ($0 \leftarrow 0$) Transition Energy Due to Substrate Binding. The fluorescence line narrowing spectra

and the site distribution results presented in Figures 5–9 and Table I indicated that all of the substrates shift the 0 ← 0 transition energy of MP toward higher energies; the energy shift of mean energy values (averaging for the tautomeric forms) are 118, 125, 145, and 195 cm^{-1} for BHA, NHA, HQ, and β-RE, respectively. In the room temperature measurements shown in Figure 2, however, the direction of the shift seems to be the opposite compared to the free protein; the fluorescence emission spectra excited at 400 nm appear at longer wavelengths for the complexed molecules. The broad-band excitation method did not show the same direction, even approaching cryogenic temperatures at 77 K; the room temperature and 77 K measurements seem to be in accordance with each other (see, e.g., results for NHA).

In Table I, the conventionally found band maxima (E^{77K}) for the free protein tautomers, NHA and β-RE, and mean values (μ) of site distributions for 0 ← 0 transition energies in the same systems can be compared. We see that in the substrate-bound cases the two energies are about equal within experimental error for the band maxima. For the free protein, however, the 0 ← 0 transition energies are located toward significantly longer wavelengths from the tautomer band maximum positions (especially for tautomer 1). Completing formula 1 by a function for broad-band excitation, the conventionally measured band position can be estimated, and it turns out to be somewhat shifted toward smaller energies related to the position of the site distribution function (Kohler, 1979); a relation may be found for the substrate-bound systems. The theoretically not acceptable large difference found for the free protein indicates that while the substrate-bound cases may be comparable at 77 K and between 5 and 40 K (range used for site selection spectra), this is not true for the free protein. It follows that we have to suppose a conformational transition in the vicinity of 77 K for free MP-HRP affecting the position (and tautomer splitting) of the site distribution function. The corresponding structural change is either missing or is of reduced effectiveness for the substrate-bound cases.

In our previous studies for free MP-HRP (Fidy et al., 1989), a conformational rearrangement between the sites was found to be activated, when the system was warmed from 5 to above 70 K, while no change in the site distribution was spectrally detected below this temperature. This result was in agreement with the concept that the energy barrier between the conformational substrates may be reduced when the temperature is increased from the cryogenic range [e.g., Frauenfelder and Young (1986) and references cited therein]; but this transition in the barrier height was found at signifiantly lower temperatures than that indicated by Mössbauer spectroscopy for myoglobin (Parak et al., 1982). The phase transition studies emphasized the significance of mobility changes of the trapped solute molecules (water) in changing the energy barriers. Both conformational changes and water mobility changes may lead to changes in the electric potential (crystal field potential) within the heme pocket, thus affecting the absolute value and splitting of tautomer 0 ← 0 energies. In MP-HRP, both parameters seem to change significantly. It is reasonable to assume that the binding of the substrate affecting both the functional freedom of the protein chain and possible shielding effects within the pocket may change some characteristic phase transition temperatures as well. However, we have to note that as the tautomer splitting was highly reduced in case of the substrate/protein complexes, this is an indication that they represent a less sensitive system for Jahn–Teller type interactions. Thus, even if the crystal field changed the same way in these cases too, it would not cause so large effect as for the free protein.

Considering the facts discussed above, we see that 77 K is probably an unfortunate temperature to compare the systems, while at cryogenic temperatures they are probably most comparable at a stage of frozen solute mobilities. We have seen in Figure 9 that the binding of substrates changes the electric potential for MP in its molecular plane; that is, conformational changes were induced within the heme pocket, which are different for the different group of substrates. In our earlier studies, we have already seen changes of MP 0 ← 0 transition energy toward higher energies, when surrounded by special matrices. Replacing the protein by diethyl ether shifted the site distribution at low temperature to 16 200 cm^{-1} (Fidy et al., 1989); in preliminary measurements on MP-myoglobin (unpublished), we found the mean energy to be around 16 330 cm^{-1}. Diethyl ether most probably provides a fairly polar, amorphous matrix for MP; from the structure of myoglobin (Frauenfelder et al., 1979) we know that in this system the porphyrin is in a rather open crevice, more accessible for water molecules. From the tendency of these two systems to shift the transition to higher energies, we conclude that the binding of the substrate may induce a conformation change that allows for stronger interactions with polar groups (water or distal histidines) to be involved in interactions with the porphyrin. The effect of substrates on the 0 ← 0 energy is around that caused by diethyl ether, and definitely less than that of myoglobin. The magnitude of the substrate energy shifting effect follows this sequence: BHA < NHA < HQ < RE's, in accordance to their arrangement on Table I.

It was mentioned in connection with Figure 7 that, in the MP-HRP/BHA case, a population of molecules characterized by structureless emission around 15950 cm^{-1} (see arrow in Figure 7A) is also represented in the emission spectra of this system. There is a moderate emission intensity within this range also for NHA (Figure 7B), but that is accountable by emissions from S_1^0 to the first (lowest energy) ground-state vibrational level (Romanovskii et al., 1981). When the effect of BHA and NHA is compared, a red shift was found (G. R. Schoenbaum, personal communication) in the room temperature absorption spectrum of BHA upon binding to native HRP, while for NHA, no significant change could be observed. We also found that, by adding more BHA above the concentrations where the spectral shift was saturated, fluorescence quenching of MP-HRP could be observed, while the complex with NHA remained characterized by the intensity of the saturation spectrum shown in Figure 2 even through much higher concentration ranges. (Among the other substrates, only γ-RE showed similar behavior to BHA in terms of fluorescence quenching.) In the literature (Morishima & Ogawa, 1979), based on NMR studies, it was suggested that BHA, in contrast to other aromatic substrates, would have two kinds of binding sites within the heme pocket of native HRP, one being close to the heme iron. Resonance Raman data indicating a sixth coordinated iron atom when BHA was added in contrast to HQ (Teraoka & Kitagawa, 1981), together with the mentioned optical spectroscopic data, support this latter model. The new band around 15 950 cm^{-1} being structureless and of lowered energy compared to the free protein indicates that BHA may also be bound out of the regular binding site in a stacking position related to the porphyrin. The amount of this type of binding is quite significant for BHA. In case of γ-RE there may be a similar reason for quenching of fluorescence; however, the low binding ability of this substrate did not allow for proving this interpretation.

Vibrational Modes. To interpret the meaning of the substrate binding effect on the S_1 vibrational modes, they should be assigned to MP vibrations. Our data can be compared with the fluorescence site selection spectrum published by Romanovskii et al. (1981) for the range of $\nu \leftarrow 0$ emissions for MP in chloroform/ether. It is certainly not evident that we can suppose mirror symmetry for emission and absorption processes for MP (where we expect a tautomeric splitting taking place in the excited state), thereby assuring the same probability relations for $S_0^0 \rightarrow S_1^\nu$ and $S_1^0 \rightarrow S_0^\nu$ vibronic transitions. We may suppose, however, that there will not be too large deformation of the molecular geometry in the excited state; that is, the intensity relations, though modified (Birks & Dyson, 1963), may not be totally inverted. This makes it possible to establish an assignment between our excited-state energies and those for ground-state vibrations using the intense 724-, 1115-, 1210-, and 1312-cm^{-1} lines from our spectra. The comparison shows an energy difference of 17–23 cm^{-1} between ground- and excited-state vibrations (the latter characterized by lower energies as in Table II). The true difference, however, may differ from this value significantly for some modes, as we neglected differences that may have arisen by the different matrices. A difference in the same direction between ground-state vibrational energies and those for the first excited triplet state of 3–7 cm^{-1} for Mg, Zn, and Pd tetraphenylporphine was reported by resonance Raman spectroscopy (Kim et al., 1986). Resonance Raman results would be relevant to assign vibrational modes to the vibronic transitions we found (Albrecht, 1961). Our data refer to the range of 700–1100 cm^{-1}; for this region very few Raman studies were performed, especially not for MP. Published fluorescence line narrowing data for the four isomeric forms of etioporphyrin (Romanovskii et al., 1981) by $0 \leftarrow 0$ excitation showed that in the studied frequency region the symmetry of the substitution plays a major role in the probability of vibronic transitions. Therefore, it is questionable to apply data gained for other porphyrins of different substitutional symmetry to the case of MP.

For comparison, resonance Raman frequencies and their assignment for Fe^{II}- and Fe^{III}-MP/$(imidazole)_2$ complexes are available for the 900–1000-cm^{-1} range (Choi & Spiro, 1983), where our studies were performed (see Table II). In listing also these published modes for comparison in Table II, we took into consideration that our data refer to the S_1 state (i.e., they appear at shorter frequencies), while the Raman frequencies characterize the S_0 electronic state, and also the fact that, because of having two tautomeric forms and an asymmetric environment around MP, we may see more modes than for metal-MP in the symmetric environment. Data for Fe^{II} and Fe^{III} complexes are both presented; although we believe that the former being of a planar configuration represents better our case, for this molecule there were even fewer data available. Thus, looking at Table II, it seems reasonable to suppose that the substrate binding effect seen in the 976–983- and the 927-cm^{-1} mode in our technique reflects the steric disturbance of a C_aN in-plane and a C_b-substituent in-plane mode, respectively. The in-plane mode of A_{1g} symmetry around 960–958 cm^{-1} did not seem to be affected by binding. It was shown (Personov, 1983) that the virtual phonon wing in fluorescence line narrowing technique is the product of the phonon wing of the excitation transition and that of the $0 \leftarrow 0$ emission. As in the measurements this latter contribution does not change; the difference originates from differences in the phonon coupling of the vibronic excitation processes. We believe that our data (in Table II and Figure 10) show a difference in the phonon coupling of a substituent-related mode for the different substrates, and a change in the energy of an inner-ring-related mode may originate from a possible deformation of the porphyrin ring upon binding (discussed also earlier in 2). The differences in the probabilities for phonon coupling go parallel with that in the $0 \leftarrow 0$ energy shifting effect, showing that they may be also of a common conformational origin.

Conclusions

The comparison of conventional and laser spectroscopic results in this paper showed that the high-resolution technique is capable of revealing details of biological processes hindered in the broad-band excitation measurements. Taking into account the temperature dependence of the conformational transitions in protein structures, we have shown that the cryogenic temperature range, 5–40 K, used in this method reduces the conformational and solvent molecular motions so that the structural changes caused by substrate binding become purely comparable. We find it especially remarkable that the method characterizes the system and the studied effect taking directly into account the existence of conformational substates. The correspondence of our experimental results to those obtained earlier by other techniques for native HRP showed that the high-resolution spectroscopic study using fluorescent derivatives of heme proteins is a promising method in the study of structural changes caused by biological processes within the heme pocket.

Our results agree with the model that the binding place for aromatic H donors in HRP is near to a propionate group of the heme in a position where the π system of the aromatic ring does not interfere with that of the porphyrin. Thus we would argue against the fact that the substrate bound to this primary site would expand toward the distal histidine as was proposed by Oertling and Babcock (1988). However, in the case of certain substrate structures, another binding place may also exist; our studies indicate a stacking interaction between this kind of bound substrate and the heme for BHA. The results allow for supposing the same for γ-RE. As the other studied aromatics do not achieve this secondary type of binding, we suppose that interactions through side chains (substituents) are also involved, maybe by forming a specific bimolecular complex with the molecule binding at the regular site.

The association constants found by us were in accordance with literature data, and the comparison with the structure of the substrates allows for some remarks. The most ideal structure for binding is that of NHA, probably because its huge delocalized π system is easily capable of stacking interactions with an aromatic binding site like the supposed tyrosine. BHA having smaller association probability shows that one aromatic ring completed with the hydroxamic acid group is not enough to fill up ideally the binding site. The poor association found for the other aromatic structures indicates that the hydroxamic acid group is also involved in binding. The outstanding capability of β-RE among the others for saturating the binding sites shows that a size somewhat smaller than BHA, with two hydrogens capable of H-bonding at the opposite ends, is a proper geometry for binding. This is supported by the case of HQ, which is although even smaller than β-RE, but having the opposite arrangements of hydrogens represents a candidate for binding. The narrow site distribution suggests the involvement of stronger bonds than only hydrophobic interactions in substrate binding as the flexibility of the protein becomes significantly reduced.

Our results revealed differences not only in the probability for binding but also in the conformation of the complexes. Upon binding, in all cases we found a significant change in

the electronic energy of the porphyrin, which was further altered by binding different aromatic substrates parallel with the change in the phonon coupling and the energy of certain vibrational modes in S_1. The electric potential field affecting the electronic transition energy in the pocket may change in different ways: (1) polar amino acid groups become rearranged; (2) some groups become shielded by taking part in new interactions; (3) the substrates or new water molecules bring new polar groups close to the heme. Our method does not differentiate between these cases, but none of them or the conformational changes behind them seem to correlate with the size of the substrate, but rather with the type of binding, that is with the side groups involved. Finally, we have to note that the loss of the significant splitting for the tautomeric forms upon all types of bindings cannot be rendered solely to a general conformational/shielding change leading to the loss of potential asymmetry for differentiating between the tautomeric forms, as even mild distortions of the planarity (symmetry) of the porphyrin may also lead to the same effect through vibronic interactions.

ACKNOWLEDGMENTS

We thank Dr. G. R. Schoenbaum and Dr. H. Frauenfelder for valuable discussions.

REFERENCES

Albrecht, A. C. (1961) *J. Chem. Phys. 34*, 1476–1484.

Angiolillo, P. J., Leigh, J. S., Jr., & Vanderkooi, J. M. (1982) *Photochem. Photobiol. 36*, 133–137.

Bersuker, I. B. (1984) in *The Jahn-Teller Effect and Vibronic Interactions in Modern Chemistry*, Plenum Press, New York.

Bersuker, I. B., & Stavrov, S. S. (1988) *Coord. Chem. Rev. 88*, 1–68.

Birks, J. B., & Dyson, D. J. (1963) *Proc. R. Soc. London, A 275*, 135–148.

Choi, S., & Spiro, T. G. (1983) *J. Am. Chem. Soc. 105*, 3683–3692.

Fidy, J., Koloczek, H., Paul, K.-G., & Vanderkooi, J. M. (1987) *Chem. Phys. Lett. 142*, 562–566.

Fidy, J., Paul, K.-G., & Vanderkooi, J. M. (1989) *J. Phys. Chem. 93*, 2253–2261.

Frauenfelder, H., & Young, R. D. (1986) *Comments Mol. Cell. Biophys. 3*, 347–372.

Frauenfelder, H., Petsko, G. A., & Tsernoglou, D. (1979) *Nature 280*, 558–563.

Fuenfschilling, J., & Zschokke-Graener, I. (1982) *Chem. Phys. Lett. 91*, 122–125.

Fuenfschilling, J., Zschokke-Granacher, I., & Williams, D. F. (1981) *J. Chem. Phys. 75*, 3670–3673.

Gurinovich, G. P., Zenkevich, E. I., & Shulga, A. M. (1986) *ACS Symp. Ser. No. 321*, 74–93.

Hoffman, B. M., & Ratner, M. A. (1978) *Mol. Phys. 35*, 901–925.

Horie, T., Vanderkooi, J. M., & Paul, K.-G. (1985) *Biochemistry 24*, 7935–7941.

Jahn, H. A., & Teller, E. (1937) *Proc. R. Soc. London, Ser. A 161*, 220.

Kim, D., Terner, J., & Spiro, T. G. (1986) *J. Am. Chem. Soc. 108*, 2097–2099.

Kohler, B. E. (1979) in *Chemical and Biochemical Applications of Lasers* (Moore, C. B., Ed.) pp 31–51, Academic Press, New York.

Koloczek, H., Fidy, J., & Vanderkooi, J. M. (1987) *J. Chem. Phys. 87*, 4388–4394.

Leigh, J. S., Maltempo, M. M., Ohlsson, P. I., & Paul, K.-G. (1975) *FEBS Lett. 51*, 305–308.

Morishima, I., & Ogawa, S. (1979) *J. Biol. Chem. 254*, 2814–2820.

Oertling, W. A., & Babcock, G. T. (1988) *Biochemistry 27*, 3331–3338.

Ohlsson, P. I., Horie, T., Vanderkooi, J. M., & Paul, K.-G. (1986) *Acta Chem. Scand., Ser. B 40*, 257–261.

Parak, F., Knapp, E. W., & Kucheida, D. (1982) *J. Mol. Biol. 161*, 177–194.

Paul, K.-G., & Ohlsson, P. I. (1978) *Acta Chem. Scand., Ser. B 32*, 395–404.

Personov, R. I. (1983) in *Spectroscopy and Excitation Dynamics of Condensed Molecular Systems* (Agranovich, V. M., & Hochstrasser, R. M., Eds.) Chapter 10, North-Holland, Amsterdam.

Romanovskii, Yu. V., Bykovskaya, L. A., & Personov, R. I. (1981) *Biophysics 26*, 631–638.

Sakurada, J., Takahashi, S., & Hosoya, T. (1986) *J. Biol. Chem. 261*, 9657–9662.

Schejter, A., Lanir, A., & Epstein, N. (1976) *Arch. Biochem. Biophys. 174*, 36–44.

Schoenbaum, G. R. (1973) *J. Biol. Chem. 248*, 502–511.

Spiro, T. G. (1983) in *Iron Porphyrins* (Lever, A. B. P., & Gray, H. B., Eds.) Part II, pp 89–152, Addison-Wesley, Reading, MA.

Teraoka, J., & Kitagawa, T. (1981) *J. Biol. Chem. 256*, 3969–3977.

Thanabal, V., La Mar, G. N., & Ropp, J. S. (1988) *Biochemistry 27*, 5400–5407.

Vanderkooi, J. M., Moy, V. T., Maniara, G., Koloczek, H., & Paul, K.-G. (1985) *Biochemistry 24*, 7931–7935.

Voelker, S., & van der Waals, J. H. (1976) *Mol. Phys. 32*, 1703–1718.